

Cite this: *Chem. Commun.*, 2012, **48**, 7483–7485

www.rsc.org/chemcomm

## Top-down patterning of Zeolitic Imidazolate Framework composite thin films by deep X-ray lithography†

Constantinos Dimitrakakis,<sup>ab</sup> Benedetta Marmiroli,<sup>c</sup> Heinz Amenitsch,<sup>c</sup> Luca Malfatti,<sup>d</sup> Plinio Innocenzi,<sup>d</sup> Gianluca Greci,<sup>e</sup> Lisa Vaccari,<sup>f</sup> Anita J. Hill,<sup>a</sup> Bradley P. Ladewig,<sup>bg</sup> Matthew R. Hill\*<sup>a</sup> and Paolo Falcaro\*<sup>a</sup>

Received 8th May 2012, Accepted 31st May 2012

DOI: 10.1039/c2cc33292b

**For the first time a top-down process was used to control the spatial location of Metal–Organic Frameworks on a surface. Deep X-ray lithography was utilised to micropattern a Zeolitic Imidazolate Framework layer on a sol–gel surface, with exposure hardening the sol–gel by inducing crosslinking while leaving the frameworks intact.**

Zeolitic Imidazolate Frameworks (ZIFs) are an exciting subclass of Metal–Organic Framework (MOF) materials, consisting of metal atoms linked in a periodic fashion by imidazolate-based ligands that adopt highly microporous structures analogous to the known zeolite networks. They exhibit very good chemical and thermal stability up to  $\sim 500$  °C<sup>1</sup> and contain pore windows of diameters within the range of 2–5 Å<sup>2</sup> owing to the 145° metal–imidazolate–metal links in the structure.<sup>3</sup> The synthesis of ZIFs typically occurs in solvents such as dimethylformamide or methanol at 100 °C or above,<sup>4</sup> although room temperature<sup>5</sup> or aqueous<sup>6</sup> syntheses are possible.

Much attention thus far has been focused on ZIFs as adsorbent materials with a view towards utilising them in mobile energy storage applications.<sup>7</sup> ZIFs are also ideally suited for gas separation owing to their large internal pore volumes and constricted pore windows, which are of a similar scale to the kinetic diameters of simple gas molecules, leading to high gas flux with good selectivity.<sup>3</sup> Initial work on adapting

ZIFs into gas-selective membranes has focused on growing them on porous inorganic supports<sup>8</sup> to produce membranes with selective layers of around 50 μm,<sup>9</sup> while novel syntheses can reduce this to as little as 100 nm.<sup>5</sup> These membranes have exhibited selectivity above that possible with polymeric membranes for separation of H<sub>2</sub> from CO<sub>2</sub>.<sup>10</sup> However, separation performance typically trends towards the natural Knudsen selectivity,<sup>11</sup> which is most likely due to the inherent pinhole or grain boundary defects present in pure inorganic layers. A polymer binder is thus desirable to reduce non-selective gas pathways in such membranes, ideally without sacrificing control of location and density of the crystal coverage.

Recent efforts have looked at creating patterned surfaces of MOFs,<sup>12</sup> and this capability would be particularly suited for the use of ZIFs in devices such as gas sensors.<sup>5</sup> To control the spatial location of MOFs on a substrate, the bottom-up approach has been the primary method used thus far.<sup>12</sup> Surface functionalisation,<sup>13–15</sup> seeding nanoparticles,<sup>16</sup> electrochemical templating,<sup>17</sup> galvanic displacement,<sup>18</sup> micro-contact printing and evaporation induced growth,<sup>19</sup> Langmuir–Blodgett<sup>20</sup> or dip-pen nanolithography<sup>21</sup> are examples of investigated approaches. These bottom-up methods all rely on intricate manipulation of surface chemistry or reaction kinetics to achieve patterned growth, potentially limiting the available combinations of framework materials, synthesis solvent and compatible surfaces. Alternatively, a top-down approach would make the patterning process independent of framework synthesis and thus allow easier application of patterning onto any desired substrate.

In this communication we present for the first time the top-down patterning of a ZIF/sol–gel composite thin film using deep X-ray lithography (DXRL). This proximity lithography<sup>22</sup> was used to selectively crosslink the sol–gel material on the regions exposed to the X-ray radiation. This approach has shown great potential for the fabrication of intricate patterns while simultaneously maintaining the functionality afforded by the ZIF.

DXRL is a promising technique for producing surface patterns on the micro- and nanoscale and can be achieved using synchrotron light sources;<sup>22</sup> other sources are currently under investigation to make a laboratory-based fabrication method viable. If a single continuous film with patterned regions is desired, a simple one-step lithography process can be sufficient.<sup>23</sup>

<sup>a</sup> Division of Materials Science and Engineering, CSIRO, Private Bag 33, Clayton South MDC 3169, Australia. E-mail: Matthew.Hill@csiro.au, Paolo.Falcaro@csiro.au; Tel: +61 3 9545 2841

<sup>b</sup> Department of Chemical Engineering, Monash University, Wellington Road, Clayton 3800, Australia

<sup>c</sup> Institute of Biophysics and Nanosystems Research, Austrian Academy of Sciences, Schmiedlstrasse 6, 8042 Graz, Austria

<sup>d</sup> Laboratorio di Scienza dei Materiali e Nanotecnologie (LMNT), CR-INSTM, Università di Sassari, Palazzo Pou Salid, Alghero, SS, Italy

<sup>e</sup> CMR-IOM, Laboratorio TASC, S.S. 14 km 163.5 Area Science Park, 34149, Basovizza, Trieste, Italy

<sup>f</sup> Sincrotrone Trieste S.C.p.A. S.S. 14, Km 163.5 Area Science Park, 34149, Basovizza, Trieste, Italy

<sup>g</sup> Leibniz Institute of Polymer Research Dresden, Hohe Strasse 6, 01069 Dresden, Germany

† Electronic supplementary information (ESI) available: Full experimental procedure, additional optical and scanning electron microscopy images, XRD patterns, FTIR data. See DOI: 10.1039/c2cc33292b

Otherwise a polymeric resist film such as polymethylmethacrylate or an epoxy resin is typically used in a two-step lithography–development process and, depending on the structural changes that occur within the resist during exposure, the exposed region can be etched away (positive resist) or becomes hardened such that the surroundings can be etched (negative resist).<sup>24</sup>

Almost all organic materials undergo a transformation through X-ray irradiation, primarily through the production of photoelectrons from the target material<sup>25</sup> which induce further chemical reactions from the propagation of free radicals.<sup>26</sup> However, the rate at which each material is affected through exposure can greatly vary. This has been exploited here, with the intention of producing a patterned gas-selective surface, by crosslinking a phenyltriethoxysilane (PhTES) sol–gel matrix heavily loaded with largely stable ZIF particles.

PhTES has been shown to exhibit a negative resist-like behaviour under hard X-ray exposure; it polymerises due to condensation reactions between silanol groups.<sup>27</sup> ZIF-9 (Co(PhIM)<sub>2</sub>, PhIM = benzimidazole) was chosen as the gas-selective component as it has been observed to exhibit a ‘breathing’ effect when exposed to changes in partial pressure of CO<sub>2</sub><sup>28</sup> while being almost completely impermeable to N<sub>2</sub><sup>29</sup> and CH<sub>4</sub>.<sup>30</sup>

Thin PhTES films were drop-cast on cleaned and dried silicon wafers from a solution of PhTES in toluene and isopropanol (Fig. 1a), the preparation of which is described elsewhere<sup>31</sup> but with the use of a closed flask to retain the solvent. The wafers were heated on a hot plate at 150 °C for 1 minute until the film was observed to have dried out (Fig. 1b). After

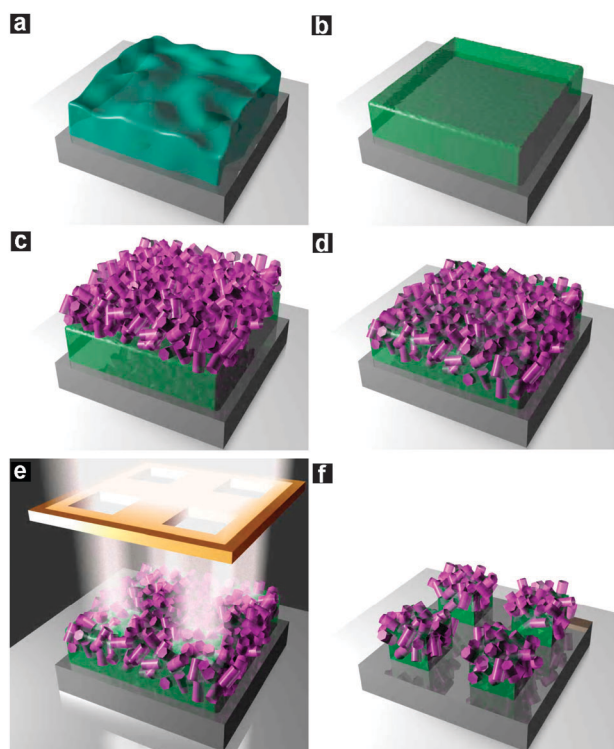


**Fig. 1** Fabrication process: phenyltriethoxysilane (PhTES) solution is drop-cast onto a silicon wafer (a) and heated until set (b). ZIF-9 powder is spread across the PhTES surface (c), heated to adhere the crystals (d) then repeated to achieve a dense coverage. The surface is then exposed to lithographic X-ray beam (e) and rinsed with ethanol, etching unexposed areas to leave behind the patterned surface (f).

cooling to room temperature in air, ZIF-9 powder was manually spread around the surface of the PhTES film to achieve a homogeneous coverage (Fig. 1c). The wafer was heated for 10 seconds during which the sol–gel layer softened<sup>32</sup> and the ZIF-9 particles were slightly sintered into a polycrystalline film which adhered to the viscous PhTES film underneath (Fig. 1d). After allowing the wafer to cool, the manual deposition and heating process was repeated until a visibly dense coating was obtained.

The samples were exposed for a limited time to synchrotron X-rays through a mask (Fig. 1e). The exposure mask was custom-built for the purpose of demonstrating the microscale etching of surfaces using deep X-rays, and featured a variety of patterns of 5 to 500 μm including microgears, hexagonal, rectangular and circular arrays and barcode patterns (see ESI†). The exposure process produced no immediate visual indication of a change in either the ZIF or the sol–gel layer. After gentle rinsing in ethanol, the unexposed regions of the PhTES layer were completely etched away, leaving behind well-defined pillars on the silica wafer surface (Fig. 1f).

Characterisation of unirradiated and irradiated (under the same X-ray exposure conditions as were used for the thin film samples) ZIF-9 powder has been performed. Little difference is observable in the powder XRD patterns of the unexposed and the exposed samples, with the pattern matching well with the theoretical XRD pattern<sup>3</sup> (see ESI†), indicating that the crystallinity of the powder samples has been preserved through the intense X-ray exposure process. Gas sorption experiments (Fig. 2) for exposed ZIF powder show that CO<sub>2</sub> uptake at 273 K is virtually unchanged, only decreasing by 3.6% at 760 mmHg, while remaining completely inaccessible to N<sub>2</sub>, but that the ‘breathing’ effect has been altered. This is consistent with an increased rigidity of the framework that may be the result of minor changes to some benzimidazole ligands due to free radicals produced during exposure; a dedicated investigation is needed in order to provide a better insight into this phenomenon.

The topography of the patterned surface is depicted in detail in Fig. 3. Optical (Fig. 3a) and SEM (Fig. 3b) imaging of the developed areas shows clearly delineated regions where the composite structure has remained intact, with the ZIF layer on top concentrated only to a depth of a few microns, demonstrating that the process maintains a dense crystalline layer supported by a hardened sol–gel substrate underneath. EDX

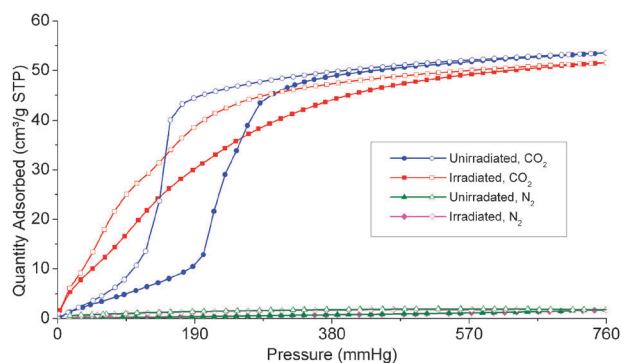


**Fig. 2** Gas sorption results at 273 K show little reduction in overall CO<sub>2</sub> uptake and selectivity over N<sub>2</sub> but uptake beginning at lower partial pressures consistent with increased framework rigidity.

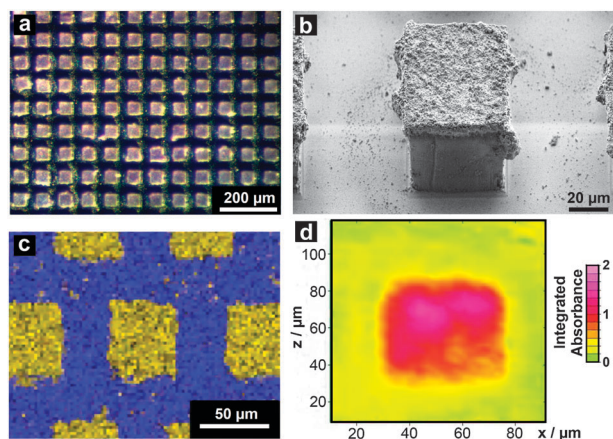


**Fig. 3** Successful patterning of a ZIF-9/PhTES composite thin film has been achieved with example patterns of sharply defined and regularly arranged  $50\ \mu\text{m} \times 50\ \mu\text{m}$  pillars imaged optically (a) and using an SEM (b). EDX surface mapping (c) of silicon (blue) and cobalt (yellow) and shows each element confined within the regular patterns, as supported by FTIR imaging (d) showing the integrated C–N stretching band ( $1310\text{--}1290\ \text{cm}^{-1}$ ).

mapping of the surface after lithography (Fig. 3c) shows that the etched areas are free of cobalt (the metal constituent of ZIF-9) while still very much concentrated on the pillars, showing that the integrity of the PhTES pillars and the ZIF layer has been maintained through the etching process. The FTIR image of a single pillar supports the EDX result by showing an intense absorption related to the C–N vibration (Fig. 3d); such a mode at about  $1300\ \text{cm}^{-1}$  is generally observed in the ZIF-9 FTIR spectra.<sup>33–35</sup>

We have shown here a new, versatile method for patterning ZIF surfaces by a top-down X-ray lithographic approach that may reduce the reliance on surface chemistry and reaction kinetics optimisation for producing patterned materials. This has been achieved through control of the irradiation conditions to ensure that the crystallinity and the adsorption capacities of ZIF-9 have been preserved, allowing this approach to potentially be applied for gas separation, sensing or transport by adapting the method to a variety of framework materials and substrates. Work to adapt this method to laboratory-based equipment is currently underway.

We acknowledge travel funding provided by the International Synchrotron Access Program (ISAP) managed by the Australian Synchrotron. The ISAP is an initiative of the Australian Government being conducted as part of the National Collaborative Research Infrastructure Strategy. CD thanks the Australian Postgraduate Award Scheme for the provision of a scholarship. PF acknowledges the Australian Research Council (ARC) for support from the DECRA Grant DE120102451 and the Advanced Materials (TCP) CSIRO scheme.

## Notes and References

- 1 Y.-S. Li, F.-Y. Liang, H. Bux, A. Feldhoff, W.-S. Yang and J. Caro, *Angew. Chem., Int. Ed.*, 2010, **49**, 548–551.
- 2 S. R. Venna and M. A. Carreon, *J. Am. Chem. Soc.*, 2009, **132**, 76–78.
- 3 K. S. Park, Z. Ni, A. P. Côté, J. Y. Choi, R. Huang, F. J. Uribe-Romo, H. K. Chae, M. O’Keeffe and O. M. Yaghi, *Proc. Natl. Acad. Sci. U. S. A.*, 2006, **103**, 10186–10191.

- 4 R. Banerjee, A. Phan, B. Wang, C. Knobler, H. Furukawa, M. O’Keeffe and O. M. Yaghi, *Science*, 2008, **319**, 939–943.
- 5 G. Lu and J. T. Hupp, *J. Am. Chem. Soc.*, 2010, **132**, 7832–7833.
- 6 Y. Pan, Y. Liu, G. Zeng, L. Zhao and Z. Lai, *Chem. Commun.*, 2011, **47**, 2071–2073.
- 7 J. L. C. Rowsell and O. M. Yaghi, *Angew. Chem., Int. Ed.*, 2005, **44**, 4670–4679.
- 8 J. Yao, D. Dong, D. Li, L. He, G. Xu and H. Wang, *Chem. Commun.*, 2011, **47**, 2559–2561.
- 9 Y. Liu, E. Hu, E. A. Khan and Z. Lai, *J. Membr. Sci.*, 2010, **353**, 36–40.
- 10 Y. Li, F. Liang, H. Bux, W. Yang and J. r. Caro, *J. Membr. Sci.*, 2010, **354**, 48–54.
- 11 A. W. Thornton, D. Dubbeldam, M. S. Liu, B. P. Ladewig, A. J. Hill and M. R. Hill, *Energy Environ. Sci.*, 2012, **5**, 7637–7646.
- 12 C. M. Doherty, D. Buso, A. J. Hill and P. Falcaro, *Adv. Mater.*, 2012, DOI: 10.1002/adma.201200485.
- 13 D. Zacher, A. Baunemann, S. Hermes and R. A. Fischer, *J. Mater. Chem.*, 2007, **17**, 2785–2792.
- 14 J.-L. Zhuang, D. Ceglarek, S. Pethuraj and A. Terfort, *Adv. Funct. Mater.*, 2011, **21**, 1442–1447.
- 15 Y. Yoo and H.-K. Jeong, *Chem. Commun.*, 2008, 2441–2443.
- 16 P. Falcaro, A. J. Hill, K. M. Nairn, J. Jasieniak, J. I. Mardel, T. J. Bastow, S. C. Mayo, M. Gimona, D. Gomez, H. J. Whitfield, R. Riccò, A. Patelli, B. Marmiroli, H. Amenitsch, T. Colson, L. Villanova and D. Buso, *Nat. Commun.*, 2011, **2**, 237.
- 17 R. Ameloot, L. Stappers, J. Fransaer, L. Alaerts, B. F. Sels and D. E. De Vos, *Chem. Mater.*, 2009, **21**, 2580–2582.
- 18 R. Ameloot, L. Pandey, M. V. d. Auweraer, L. Alaerts, B. F. Sels and D. E. De Vos, *Chem. Commun.*, 2010, **46**, 3735–3737.
- 19 R. Ameloot, E. Gobechiya, H. Uji-i, J. A. Martens, J. Hofkens, L. Alaerts, B. F. Sels and D. E. De Vos, *Adv. Mater.*, 2010, **22**, 2685–2688.
- 20 M. Tsotsalas, A. Umemura, F. Kim, Y. Sakata, J. Reboul, S. Kitagawa and S. Furukawa, *J. Mater. Chem.*, 2012, **22**, 10159–10165.
- 21 C. Carbonell, I. Imaz and D. MasPOCH, *J. Am. Chem. Soc.*, 2011, **133**, 2144–2147.
- 22 P. Innocenzi, L. Malfatti and P. Falcaro, *Soft Matter*, 2012, **8**, 3722–3729.
- 23 P. Falcaro, L. Malfatti, L. Vaccari, H. Amenitsch, B. Marmiroli, G. Grecni and P. Innocenzi, *Adv. Mater.*, 2009, **21**, 4932–4936.
- 24 S. Costacurta, L. Malfatti, A. Patelli, P. Falcaro, H. Amenitsch, B. Marmiroli, G. Grecni, M. Piccinini and P. Innocenzi, *Plasma Processes Polym.*, 2010, **7**, 459–465.
- 25 F. Cerrina, in *Handbook of microlithography, micromachining, and microfabrication*, ed. P. Rai-Choudhury, SPIE, Bellingham, Washington, USA, 1997, pp. 251–320.
- 26 P. Meyer, J. Schulz and V. Saile, in *Micromanufacturing Engineering and Technology*, ed. Y. Qin, Elsevier, Oxford, UK, 2010, pp. 202–220.
- 27 P. Innocenzi, L. Malfatti, T. Kidchob, S. Costacurta, P. Falcaro, B. Marmiroli, F. Cacho-Nerin and H. Amenitsch, *J. Synchrotron Radiat.*, 2011, **18**, 280–286.
- 28 S. Aguado, G. Bergeret, M. P. Titus, V. Moizan, C. Nieto-Draghi, N. Bats and D. Farrusseng, *New J. Chem.*, 2011, **35**, 546–550.
- 29 ExxonMobil Research and Engineering Company, *US Pat.*, 8142745, 2012.
- 30 ExxonMobil Research and Engineering Company, *US Pat.*, 8142746, 2012.
- 31 P. Falcaro, S. Costacurta, L. Malfatti, D. Buso, A. Patelli, P. Schiavuta, M. Piccinini, G. Grecni, B. Marmiroli, H. Amenitsch and P. Innocenzi, *ACS Appl. Mater. Interfaces*, 2011, **3**, 245–251.
- 32 H. Kakiuchida, M. Takahashi, Y. Tokuda, H. Masai, M. Kuniyoshi and T. Yoko, *J. Phys. Chem. B*, 2006, **110**, 7321–7327.
- 33 J. C. Tan, T. D. Bennett and A. K. Cheetham, *Proc. Natl. Acad. Sci. U. S. A.*, 2010, **107**, 9938–9943.
- 34 S. Mohan, N. Sundaraganesan and J. Mink, *Spectrochim. Acta, Part A*, 1991, **47**, 1111–1115.
- 35 L. T. L. Nguyen, K. K. A. Le, H. X. Truong and N. T. S. Phan, *Catal. Sci. Technol.*, 2012, **2**, 521–528.